Direct and indirect methods in optimal control with state constraints and the climbing trajectory of an aircraft

Olivier Cots, Joseph Gergaud, Damien Goubinat

Research report IRIT/RR–2016–11–FR, September 9, 2016
URL: http://cots.perso.enseeiht.fr

Direct and indirect methods in optimal control with state constraints and the climbing trajectory of an aircraft

O. Cots[1], J. Gergaud[1] and D. Goubinat[2*]

[1]*Toulouse Univ., INP-ENSEEIHT, IRIT & CNRS, 2 rue Camichel, F-31071 Toulouse, France*
[2]*Thales Avionics SA, 105 av du General Eisenhower, B.P. 1147, 31047 Toulouse Cedex, France*

SUMMARY

In this article, the minimum time and fuel consumption of an aircraft in its climbing phase is studied using direct and indirect schemes implemented in the *Bocop* and *HamPath* softwares. The controls are the thrust and the lift and state constraints are taken into account: air slope and speed limitations. The indirect method is the numerical implementation of the Maximum Principle with state-constraints and it is initialized by the direct method. This leads to describe, for prescribed boundary conditions, extremals which satisfy necessary conditions of optimality with at most two boundary arcs.

KEY WORDS: Geometric optimal control; state constraints; direct and indirect methods; aircraft trajectory.

1. INTRODUCTION

A flight is composed of several phases which are take-off, climb, cruise, descent, approach and landing, see Figure 1. In this article, we are interested in the optimal control of an aircraft during its climbing phase. This phase is determined by its own dynamics given by an ordinary differential equation, constraints to comply with and a criterion to minimize. The climbing phase has already been studied in [2, 16] with different models and state constraints are not taken into account. Companies are trying to optimize the cost of the flight which is a combination of fuel consumption, time of flight and some environmental issues as noise. In this study, we define the objective function by a weighted sum of the two criteria: time of flight and fuel consumption.

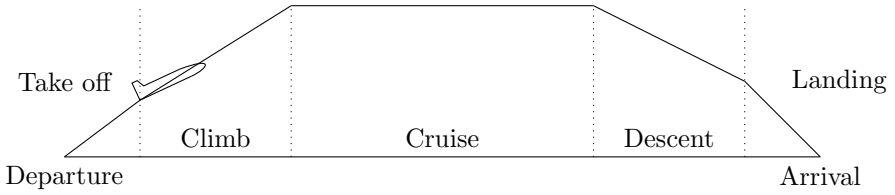

Figure 1. A flight divided into phases

The solution of the optimal control problem can be found as an extremal solution of the maximum principle with state constraints. The associated optimal strategy is a concatenation of boundary and interior arcs. Each type of arc is fully determined by the application of the maximum principle and

*Correspondence to: Thales Avionics SA, 105 av du General Eisenhower, B.P. 1147, 31047 Toulouse Cedex, France. E-mail: damien.goubinat@enseeiht.fr

we use the direct method to get the structure of the optimal trajectory. For a given structure, the application of the maximum principle leads to the formulation of a Multi Point Boundary Value Problem (MPBVP). Solving the MPBVP gives an extremal which satisfies the necessary conditions of optimality. The MPBVP can be written as a set of non linear equations which are solved by a Newton-like algorithm. The sensitivy of Newton algorithms with respect to the initial guess is well known and we use the result from the direct method – this is justify by proposition 4.1 – as starting guess.

The paper is organized as follows. The physical model with the optimal control problem are defined in section 2. We give preliminary numerical results from the direct method at the end of this section. This gives an insight into the optimal structures. In section 3, we analyze the optimal control problem with the application of the maximum principle with phase constraints. Then numerical algorithms and results are presented in section 4. Section 5 concludes the article.

2. PHYSICAL MODEL AND MAYER OPTIMAL CONTROL PROBLEM

2.1. Aircraft performance model

In this section, the aircraft dynamics equation is presented. A non linear point-mass representation is used. An aircraft is subjected to four forces, its own weight $\overrightarrow{P}$, the Lift $\overrightarrow{L}$ which compensate the weight of the aircraft, the Thrust $\overrightarrow{T}$ which we consider colinear to the velocity vector $\overrightarrow{V}$ and the Drag force $\overrightarrow{D}$ which corresponds to friction between the aircraft and the air, see Figure 2.

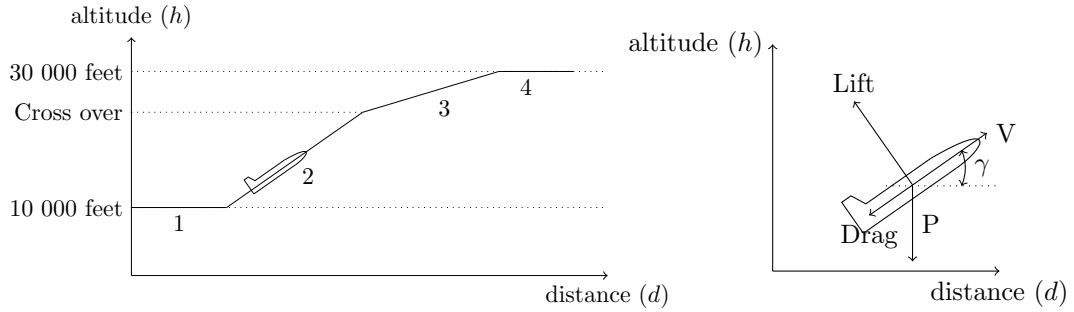

Figure 2. (a): A typical climb procedure, (1) the aircraft increases its speed at constant altitude. (2) Once it reaches its climbing speed, it starts to climb until reaching cross over altitude. (3) after reaching the cross over altitude, the aircraft follows a trajectory at constant mach speed. (4) Finally, the aircraft reaches its cruise altitude. (b): Forces representation. The angle between the Thrust and the velocity vector is ignored.

The first Dynamic Principle provides the equations of motion of this aircraft with respect to t.

$$\begin{aligned}
\frac{\mathrm{d}h}{\mathrm{d}t}(t) &= V(t)\sin(\gamma(t)) \\
\frac{\mathrm{d}d}{\mathrm{d}t}(t) &= V(t)\cos(\gamma(t)) \\
m(t)\frac{\mathrm{d}V}{\mathrm{d}t}(t) &= \varepsilon T_{\max}(h(t)) - \frac{1}{2}\rho(h(t))SV(t)^2 C_D(C_L) - m(t)g\sin(\gamma(t)) \\
\frac{\mathrm{d}m}{\mathrm{d}t}(t) &= -\varepsilon C_s(V(t))T_{\max}(h(t)) \\
m(t)V(t)\frac{\mathrm{d}\gamma}{\mathrm{d}t}(t) &= \frac{1}{2}\rho(h(t))SV(t)^2 C_L - m(t)g\cos(\gamma(t))
\end{aligned} \tag{1}$$

The description of the parameters is given in Table I. To represent air density ρ, temperature Θ and pressure P as smooth functions of altitude h, we use the smooth *International Standard Atmosphere* (ISA) model. In this study, altitude will not be higher than 11 000 meters, so we could restrain ISA

Parameter	Description	Unit
h	Altitude	m
d	Longitudinal distance	m
V	True air speed	m.s^{-1}
m	Aircraft mass	kg
γ	Air slope	
$T_{\max}$	Maximum thrust	N
C_s	Fuel flow model	kg.N^{-1}.s^{-1}
S	Wing area	m.s^2
ρ	Air density	kg.m^{-3}
g	Gravitational constant (assume to be constant)	m.s^{-2}
C_L	Lift coefficient	
C_D	Drag coefficient	
ε	Ratio of maximum thrust	

Table I. Description of the data from aircraft dynamics.

model to:

$$\Theta(h) \coloneqq \Theta_0 - \beta h, \quad P(h) \coloneqq P_0 \left(\frac{\Theta(h)}{\Theta_0}\right)^{\frac{g}{\beta R}} \quad \text{and} \quad \rho(h) \coloneqq \frac{P(h)}{R\Theta(h)}.$$

We also use the *BADA* model [17] from EUROCONTROL which provides a general smooth aircraft performance model and specific values of coefficients, depending on the type of the aircraft:

$$\begin{aligned} T_{\max}(h) &\coloneqq C_{T_1}\left(1 - \frac{h}{C_{T_2}} + C_{T_3}h^2\right), \\ C_s(V) &\coloneqq C_{s_1}\left(1 + \frac{V}{C_{s_2}}\right), \\ C_D(C_L) &\coloneqq C_{D_1} + C_{D_2}{C_L}^2. \end{aligned}$$

The description of the parameters from ISA and BADA models is given in Table. II.

Parameter	Description	Unit
P_0	Standard pressure	Pa
Θ_0	Standard temperature	K
R	Perfect gases constant	J.kg^{-1}.K^{-1}
β	Variation of temperature w.r.t altitude	K.m^{-1}
C_{T_1}	Aicraft specific data for thrust	N
C_{T_2}	Aicraft specific data for thrust	m
C_{T_3}	Aicraft specific data for thrust	m^{-2}
C_{s_1}	Aicraft specific data for fuel flow	kg.N^{-1}.s^{-1}
C_{s_2}	Aicraft specific data for fuel flow	m.s^{-1}
C_{D_1}, C_{D_2}	Aircraft specific data for drag	
γ_{air}	Heat capacity ratio of air	
$\mu \coloneqq \frac{\gamma_{\text{air}}-1}{\gamma_{\text{air}}}$	Constant derived from Heat capacity ratio	

Table II. Description of the parameters from ISA and BADA models.

The aircraft evolves in a constrained context: these contraints arise from *air traffic control* (ATC) or physical limitations. In order to protect the structure of the aircraft its speed is limited. As it is difficult to compute the real speed, a *Computed Air Speed* (CAS) which is given by a *Pitot tube*

is used and limited by the *Operation Maximal Speed* (VMO), see eq. (2). Beyond a given altitude, *Mach* speed is usually used and limited by the *Maximal Mach Operation* (MMO), see eq. (3). Other constraints are coming from ATC. For example, in a climbing phase the aircraft is not allowed to go down ($\gamma \geq 0$) and to avoid the stall of the aircraft the air slope is limited ($\gamma \leqslant \gamma_{\max}$). Only the constraints arising from the air slope and the Mach speed will be taken into account in this study:

$$CAS \coloneqq \sqrt{\frac{2P_0}{\mu\,\rho(0)}\left(\left(\frac{P(h)}{P_0}\left(\left[\frac{\mu V^2}{2R\,\Theta(h)}+1\right]^{\frac{1}{\mu}}-1\right)+1\right)^{\mu}-1\right)} \leqslant VMO, \tag{2}$$

$$M \coloneqq \frac{V}{a(h)} = \frac{V}{\sqrt{\gamma_{\text{air}}\,R\,\Theta(h)}} \leqslant MMO. \tag{3}$$

2.2. Mayer formulation of the optimal control problem

Let note $x \coloneqq (h, d, V, m, \gamma)$ the state, $M \coloneqq \mathbb{R}^5$ the state space, $u \coloneqq (\varepsilon, C_L)$ the control, $U \coloneqq \{u = (u_1, u_2) \in \mathbb{R}^2, u_i \in [u_{i,\min}, u_{i,\max}], i = 1, 2\}$ the control domain. We put all constant data in a vector ω which belongs to $\mathbb{R}^{15}$:

$$\omega \coloneqq \big(S, g, C_{T_1}, C_{T_2}, C_{T_3}, C_{D_1}, C_{D_2}, C_{s_1}, C_{s_2}, R, \Theta_0, \beta, P_0, \mu, \gamma_{\text{air}}\big),$$

with $\omega_i > 0$, $i = 1, \ldots, 15$. The values of the parameters are given in Table III in section 2.3. The dynamics from eq. (1) can be written in the form

$$f(x(t), u(t)) \coloneqq f_0(x(t)) + u_1(t) f_1(x(t)) + u_2(t) f_2(x(t)) + u_2(t)^2 f_3(x(t)),$$

where f_0, f_1, f_2 and f_3 are the following smooth vector fields:

$$\begin{aligned}
f_0(x) &\coloneqq x_3\big(\sin(x_5)\frac{\partial}{\partial x_1} + \cos(x_5)\frac{\partial}{\partial x_2}\big) - \big(\omega_6\,\theta_3(x,\omega) + \omega_2\sin(x_5)\big)\frac{\partial}{\partial x_3} - \frac{\omega_2}{x_3}\cos(x_5)\frac{\partial}{\partial x_5},\\
f_1(x) &\coloneqq \frac{\theta_1(x,\omega)}{x_4}\frac{\partial}{\partial x_3} - \theta_1(x,\omega)\,\theta_2(x,\omega)\frac{\partial}{\partial x_4},\\
f_2(x) &\coloneqq \frac{\theta_3(x,\omega)}{x_3}\frac{\partial}{\partial x_5},\\
f_3(x) &\coloneqq -\omega_7\,\theta_3(x,\omega)\frac{\partial}{\partial x_3},
\end{aligned}$$

and where $\theta(x,\omega) \coloneqq (\theta_1(x,\omega), \theta_2(x,\omega), \theta_3(x,\omega), \theta_4(x,\omega), \theta_5(x,\omega))$ is a vector of auxiliary functions with

$$\begin{aligned}
&\theta_1(x,\omega) \coloneqq \omega_3\left(1 - \frac{x_1}{\omega_4} + \omega_5 x_1^2\right), \quad \theta_2(x,\omega) \coloneqq \omega_8\left(1 + \frac{x_3}{\omega_9}\right), \quad \theta_3(x,\omega) \coloneqq \frac{\omega_1\,x_3^2\,\theta_5}{2\,\omega_{10}\,x_4\,\theta_4},\\
&\theta_4(x,\omega) \coloneqq \omega_{11} - \omega_{12}\,x_1, \quad \theta_5(x,\omega) \coloneqq \omega_{13}\left(\frac{\theta_4}{\omega_{11}}\right)^{\frac{\omega_2}{\omega_{10}\omega_{12}}}.
\end{aligned}$$

The climbing phase starts from the fixed initial state $x_0 \coloneqq (h_0, d_0, V_0, m_0, \gamma_0) \in M$ and stops when the state reaches the terminal submanifold $M_f \coloneqq \{x \in M,\ b(x) = 0\}$, with

$$b(x) \coloneqq \begin{pmatrix} x_1 - x_{1,f} \\ x_2 - x_{2,f} \\ x_3 - x_{3,f} \\ x_5 - x_{5,f} \end{pmatrix},$$

where $x_{1,f}$, $x_{2,f}$, $x_{3,f}$ and $x_{5,f}$ are fixed final conditions. The final mass is free. The state constraints the aircraft has to satisfy all along the trajectory, see subsection 2.1, are put together in a vector of

constraints c defined by

$$c(x) \coloneqq \begin{pmatrix} x_{5,\min} - x_5 \\ \psi(x) - \psi_{\max} \end{pmatrix}, \quad \text{with} \quad \psi(x) \coloneqq \frac{x_3}{\sqrt{\omega_{15}\,\omega_{10}\,\theta_4(x,\omega)}}.$$

The two main contributors which cost to a company during a flight are the fuel consumption and the flight duration. That is why we are interested in a mixed objective function which combines these two contributors. Finally, the optimal control problem can be summarized this way:

$$(\mathcal{P}_\alpha) \quad \begin{cases} g_\alpha(t_f, x(t_f)) \coloneqq (1-\alpha)\,(x_{0,4} - x_4(t_f)) + \alpha\, t_f \longrightarrow \min\limits_{t_f, u(\cdot)}, \quad \alpha \in [0,1] \text{ fixed}, \\ \dot{x}(t) = f(x(t), u(t)), \quad u(t) \in U, \quad t \in [0, t_f] \textit{ a.e.}, \quad t_f > 0, \\ x(0) = x_0, \\ c_i(x(t)) \leqslant 0, \quad i = 1, 2, \quad t \in [0, t_f], \\ b(x(t_f)) = 0. \end{cases}$$

2.3. Preliminary numerical results

We give in this section some preliminary results on the structures of the trajectories for two different problems: $\alpha = 1$ (minimum time problem) and $\alpha = 0.6$, for a medium-haul aircraft, see Table III. For each problem we compare the strategies for both the state constrained and the state unconstrained cases. In the state unconstrained case, we simply remove the constraints $c_i(x(t)) \leqslant 0$, $i = 1, 2$. We use a direct method within the *Bocop* software [3], see section 4, to get the following numerical results.

On Figure 3 (resp. 4), we display the values of the constraints and the controls along the trajectories solution of problem $(\mathcal{P}_1)$ (resp. $(\mathcal{P}_{0.6})$) for both cases: with and without taking into account the state constraints. We can see that the constraint on the air slope $c_\gamma(x) \coloneqq x_{5,\min} - x_5(x)$ is necessary for both problems whereas the constraint on the Mach speed $c_v(x) \coloneqq \psi(x) - \psi_{\max}$ comes up only in problem $(\mathcal{P}_{0.6})$. Note that these two constraints are not active simultaneously.

Remark 1. In this paper, we restrict the theoretical study to the observations from this section.

Parameter	Value	Parameter	Value
ω_1	122.6	$x_{1,0}$	3480
ω_2	9.81	$x_{2,0}$	0
ω_3	141040	$x_{3,0}$	151.67
ω_4	14909.9	$x_{4,0}$	$\in [4.8 \times 10^4, 7.6 \times 10^4]$
ω_5	$6.997{\times}10^{-10}$	$x_{5,0}$	0.07
ω_6	0.0242	$x_{1,\mathrm{f}}$	9144
ω_7	0.0469	$x_{2,\mathrm{f}}$	150 000
ω_8	$1.055{\times}10^{-5}$	$x_{3,\mathrm{f}}$	191.0
ω_9	441.54	$x_{5,\mathrm{f}}$	0
ω_{10}	287.058	$\psi_{\max}$	0.82
ω_{11}	288.15	$x_{5,\min}$	0
ω_{12}	0.0065	$u_{1,\min}$	0.3
ω_{13}	101325	$u_{2,\min}$	0
ω_{14}	0.2857	$u_{1,\max}$	1
ω_{15}	1.4	$u_{2,\max}$	1.6

Table III. Values of the constant parameters.

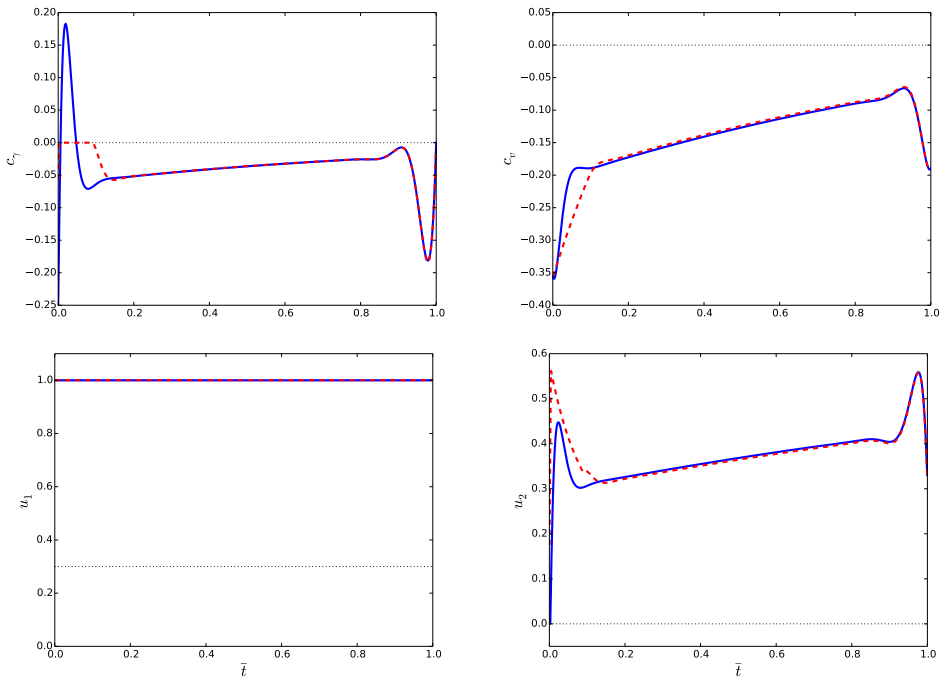

Figure 3. Evolution of the constraints and the controls along a time minimum trajectory ($\alpha = 1$) with respect to the normalized time $\bar{t}$. The red dashed lines represent problem $(\mathcal{P}_1)$ while the same problem without state constraints is represented by blue solid lines. The boundaries of state and control constraints are given by the dotted horizontal lines.

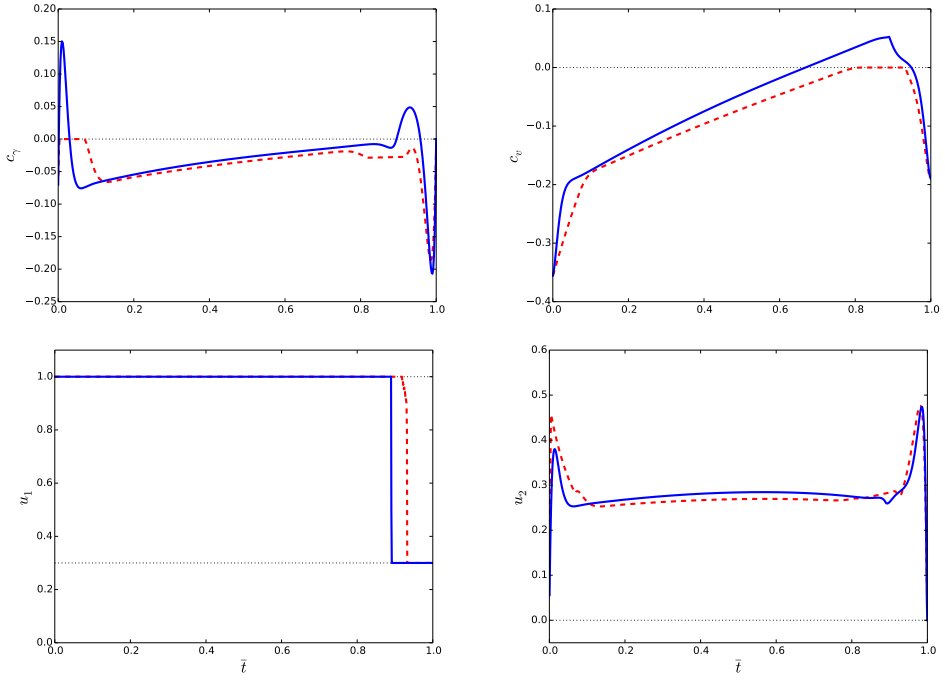

Figure 4. Evolution of the constraints and the controls along a time minimum trajectory ($\alpha = 0.6$) with respect to the normalized time $\bar{t}$. The red dashed lines represent problem $(\mathcal{P}_{0.6})$ while the same problem without state constraints is represented by blue solid lines. The boundaries of state and control constraints are given by the dotted horizontal lines.

3. ANALYSIS OF PROBLEM ($\mathcal{P}_\alpha$) WITH MAXIMUM PRINCIPLE WITH PHASE CONSTRAINTS

3.1. Necessary optimality conditions

Let define the pseudo-Hamiltonian of the *Mayer* optimal control problem ($\mathcal{P}_\alpha$) by

$$\begin{aligned} H\colon T^*M \times U \times \mathbb{R}^2 &\longrightarrow \mathbb{R} \\ (x,p,u,\eta) &\longmapsto H(x,p,u,\eta) \coloneqq \langle p, f(x,u)\rangle + \langle \eta, c(x)\rangle \end{aligned}$$

where T^*M is the cotangent bundle of M and η is the Lagrange multiplier associated to the constraint vector $c(x)$. If $(u^*(\cdot), t_f^*)$ is optimal with $x^*(\cdot)$ the associated optimal trajectory, then under some regularity assumptions, the *maximum principle* [12, 13, 18] asserts that there exists a real number $p^0 \leqslant 0$ and a function $p^*(\cdot)$ of bounded variation such that $(p^*(\cdot), p^0) \neq (0,0)$. Besides, there exists a function $\eta^*(\cdot)$ such that $\eta_i^*(t) \leqslant 0$ and $\eta_i^*(t)\, c_i(x^*(t)) = 0$, $i = 1, 2$, for all t in $[0, t_f^*]$. Moreover, we have for almost every $t \in [0, t_f^*]$

$$\dot{x}^*(t) = \frac{\partial H}{\partial p}(x^*(t), p^*(t), u^*(t), \eta^*(t)), \quad \dot{p}^*(t) = -\frac{\partial H}{\partial x}(x^*(t), p^*(t), u^*(t), \eta^*(t)) \tag{4}$$

and we have the maximization condition

$$H(x^*(t), p^*(t), u^*(t), \eta^*(t)) = \max_{u \in U} H(x^*(t), p^*(t), u, \eta^*(t)). \tag{5}$$

The boundary conditions must be fulfilled and we have the following transversality conditions:

$$p^*(t_f^*) = p^0 \frac{\partial g_\alpha}{\partial x}(t_f^*, x^*(t_f^*)) + \sum_{k=1}^{4} \lambda_k\, b_k'(x^*(t_f^*)), \quad (\lambda_1, \ldots, \lambda_4) \in \mathbb{R}^4 \tag{6}$$

Since the final time t_f^* is free, if $u^*(\cdot)$ is continuous at time t_f^*, we have:

$$H[t_f^*] = -p^0 \frac{\partial g_\alpha}{\partial t}(t_f^*, x^*(t_f^*)), \tag{7}$$

where $[t]$ stands for $(x^*(t), p^*(t), u^*(t), \eta^*(t))$. Let $\mathcal{T}$ denote the set of contact and junction[†] times with the boundary. Then at $\tau \in \mathcal{T}$ we have

$$H[\tau^+] = H[\tau^-], \tag{8}$$

$$p(\tau^+) = p(\tau^-) - \nu_{i,\tau}\, c_i'(x(\tau)), \quad \nu_{i,\tau} \leqslant 0, \quad i = 1, 2. \tag{9}$$

Remark 2. Either $p^0 = 0$ (*abnormal case*), or p^0 can be set to -1 by homogeneity (*normal case*). We consider only the normal case.

Definition 1. We call an *extremal* the quadruplet $(x(\cdot), p(\cdot), u(\cdot), \eta(\cdot))$ defined on $[0, t_f]$ where $u(\cdot)$ is an admissible control[‡] and which satisfies eqs. (4), (5), (8), (9). Any extremal satisfying the boundary conditions and equations (6), (7) is called a *BC-extremal*. We define the *Hamiltonian lifts* $H_i(z) \coloneqq \langle p, f_i(x)\rangle$, $i = 1, \ldots, 4$, $z \coloneqq (x, p)$, and the function $\varphi(t) \coloneqq \frac{\partial H}{\partial u}(z(t), u(t), \eta(t)) = (\varphi_1(t), \varphi_2(t))$, with $\varphi_1(t) = H_1(z(t))$ and $\varphi_2(t) = H_2(z(t)) + 2\, u_2(t)\, H_3(z(t))$.

[†] A junction time is either an entry or an exit time of a boundary arc. A contact time is a time when the arc has an isolated contact with the boundary.

[‡] An admissible control is a L^∞-mappings on $[0, t_f]$ taking its values in U such that the associated trajectory $x(\cdot)$ is globally defined on $[0, t_f]$.

3.2. Adjoint equations and transversality conditions

Using conditions (4), we get the adjoint equations[§]:

$$
\begin{aligned}
\dot{p}_1 &= p_3\frac{\theta_3}{\theta_4}(\omega_{12}-\frac{\omega_2}{\omega_{10}})(\omega_6+u_2^2\omega_7)-u_1\omega_3(\frac{p_3}{x_4}-p_4\theta_2)(-\frac{1}{\omega_4}+2\omega_5x_1)\\
&\quad -p_5\frac{u_2}{x_3}\frac{\theta_3}{\theta_4}(\omega_{12}-\frac{\omega_2}{\omega_{10}})-\langle\eta,\frac{\partial c}{\partial x_1}\rangle,\\
\dot{p}_2 &= 0,\\
\dot{p}_3 &= -p_1\sin(x_5)-p_2\cos(x_5)+2p_3\frac{\theta_3}{x_3}\left(\omega_6+u_2^2\omega_7\right)+p_4\theta_1\frac{\omega_8}{\omega_9}u_1\\
&\quad -\frac{p_5}{x_3^2}\left(u_2\theta_3+\omega_2\cos(x_5)\right)-\langle\eta,\frac{\partial c}{\partial x_3}\rangle,\\
\dot{p}_4 &= -p_3\frac{\theta_3}{x_4}\left(\omega_6+\omega_7u_2^2\right)+p_3\frac{\theta_1}{x_4^2}u_1+p_5\frac{\theta_3}{x_3x_4}u_2-\langle\eta,\frac{\partial c}{\partial x_4}\rangle,\\
\dot{p}_5 &= x_3(-p_1\cos(x_5)+p_2\sin(x_5))+p_3\omega_2\cos(x_5)-p_5\frac{\omega_2}{x_3}\sin(x_5)-\langle\eta,\frac{\partial c}{\partial x_5}\rangle.
\end{aligned}
\tag{10}
$$

From equations (6) and (7) we have $p_4^*(t_f^*)=p^0(\alpha-1)$ and $H[t_f^*]=-p^0\alpha$. Since the system is autonomous, the Hamiltonian is constant along any extremal and then $H[t]=-p^0\alpha$, $t\in[0,t_f]$ *a.e.*

3.3. Lie bracket definition

3.3.1. Notation

If f is a smooth function on M and X is a smooth vector field on M, X acts on f by the *Lie derivative* $f\mapsto X\cdot f$ with $(X\cdot f)(x)\coloneqq f'(x)X(x)$. Considering two smooth vector fields X_0 and X_1, the operator $X_1\mapsto[X_0,X_1]\coloneqq X_0\cdot X_1-X_1\cdot X_0$ gives the *Lie bracket* on vector fields. The *Poisson bracket* of the two Hamiltonian lifts H_0 and H_1 of X_0 and X_1 is defined by $\{H_0,H_1\}\coloneqq\overrightarrow{H}_0\cdot H_1$ where $\overrightarrow{H}_0\coloneqq(\partial_pH_0,-\partial_xH_0)$. We use the notation H_{01} (resp. X_{01}) to denote the bracket $\{H_0,H_1\}$ (resp. $[X_0,X_1]$). Since H_0 and H_1 are two Hamiltonian lifts, $\{H_0,H_1\}=\langle p,[X_0,X_1]\rangle$.

3.3.2. Computations of Lie brackets

Let introduce the vector field

$$
\begin{aligned}
f_{02}(x) &= -\theta_3\cos(x_5)\frac{\partial}{\partial x_1}+\theta_3\sin(x_5)\frac{\partial}{\partial x_2}+\frac{\omega_2\theta_3}{x_3}\cos(x_5)\frac{\partial}{\partial x_3}\\
&\quad +\left(\frac{\theta_3}{\theta_4}\left(\omega_{12}-\frac{\omega_2}{\omega_{10}}\right)\sin(x_5)-\frac{\theta_3}{x_3^2}\left(\omega_6\theta_3+2\omega_2\sin(x_5)\right)\right)\frac{\partial}{\partial x_5},
\end{aligned}
$$

then we have the following proposition.

Proposition 3.1. *The vector set* $(f_0(x),f_1(x),f_2(x),f_3(x),f_{20}(x))$ *forms a basis of* T_xM *for every* $x\in M_1\coloneqq\{x\in M,\ x_1\neq\frac{\omega_{11}}{\omega_{12}},\ x_1\neq\frac{1\pm\sqrt{1-4\omega_4^2\omega_5}}{2\omega_4\omega_5},\ x_3\neq0,\ x_3\neq-\omega_9,\ x_4\neq0\}$.

Proof
We have $\det\left(f_0(x),f_1(x),f_2(x),f_3(x),f_{02}(x)\right)=-\omega_7\theta_1\theta_2\theta_3^3\neq0$ for $x\in M_1$. □

In our problem, quantities θ_1, θ_2 and θ_3 could not be equal to zero due to physical considerations, so any trajectory $x(\cdot)$ belongs to M_1 and we can express all the Lie brackets on the basis previously defined. Brackets of order two are then:

$$
f_{01}=a_{01}f_0+b_{01}f_1+d_{01}f_2+e_{01}f_3,\quad f_{03}=a_{03}f_0+d_{03}f_2+e_{03}f_3,
$$

[§]If necessary, we omit arguments of the functions for readibility.

$$f_{21} = d_{21} f_2, \quad f_{31} = b_{31} f_1 + e_{31} f_3, \quad f_{23} = d_{23} f_2,$$

where

- $a_{01} = -\dfrac{\theta_1}{x_3 x_4},$
- $b_{01} = \omega_3 \dfrac{x_3}{\theta_1}\left(-\dfrac{1}{\omega_4} + 2\omega_5 x_1\right)\sin(x_5) - \dfrac{1}{\theta_2}\dfrac{\omega_8}{\omega_9}\left(\omega_6\theta_3 + \omega_2\sin(x_5)\right),$
- $d_{01} = -\dfrac{2}{x_3 x_4}\dfrac{\theta_1}{\theta_3}\omega_2\cos(x_5),$
- $e_{01} = -2\dfrac{\theta_1}{x_3 x_4}\dfrac{\omega_6}{\omega_7} - \dfrac{\theta_1\theta_2}{x_4}\dfrac{\omega_6}{\omega_7} + \dfrac{1}{\omega_7}\dfrac{\theta_1}{\theta_3 x_4}\left(\omega_6\theta_3 + \omega_2\sin(x_5)\right)\left(\dfrac{1}{x_3} - \dfrac{\omega_8}{\omega_9\theta_2}\right),$
- $a_{03} = \omega_7\dfrac{\theta_3}{x_3},$
- $d_{03} = 2\dfrac{\omega_2\omega_7}{x_3}\cos(x_5),$
- $e_{03} = -\omega_6\dfrac{\theta_3}{x_3} + \left(\dfrac{x_3}{\theta_4}\left(\omega_{12} - \dfrac{\omega_2}{\omega_{10}}\right) - 3\dfrac{\omega_2}{x_3}\right)\sin(x_5),$
- $d_{21} = -\dfrac{\theta_1}{x_4}\left(\dfrac{1}{x_3} + \theta_2\right),$
- $b_{31} = -\dfrac{\omega_7\omega_8}{\omega_9}\dfrac{\theta_3}{\theta_2},$
- $e_{31} = -\dfrac{\theta_1}{x_4}\left(\theta_2 + \dfrac{2}{x_3} + \dfrac{\omega_8}{\omega_9\theta_2}\right),$
- $d_{23} = \omega_7\dfrac{\theta_3}{x_3}.$

3.4. Parameterization of extremal curves (state unconstrained case)

Let consider first the state unconstrained case. We denote by $\bar{u}_2(z) := -H_2(z)/2H_3(z)$, the value that cancels φ_2. Hence the controls that maximize the Hamiltonian are given by:

$$u_1(z) = \begin{cases} u_{1,\max}, \text{ if } H_1(z) > 0, \\ u_{1,\min}, \text{ if } H_1(z) < 0, \\ u_{1,s}(z) \in [u_{1,\min}, u_{1,\max}], \text{ if } H_1(z) = 0, \end{cases}$$

and

- if $H_3(z) > 0$, then $u_2(z) = \arg\max(H(u_{2,\min}), H(u_{2,\max}))$,
- if $H_3(z) < 0$, then $u_2(z) = \begin{cases} u_{2,\max}, \text{ if } \bar{u}_2(z) > u_{2,\max}, \\ u_{2,\min}, \text{ if } \bar{u}_2(z) < u_{2,\min}, \\ \bar{u}_2(z), \text{ if } \bar{u}_2(z) \in [u_{2,\min}, u_{2,\max}], \end{cases}$
- if $H_3(z) = 0$, then $u_2(z) = \begin{cases} u_{2,\max}, \text{ if } H_2(z) > 0, \\ u_{2,\min}, \text{ if } H_2(z) < 0, \\ u_{2,s}(z) \in [u_{2,\min}, u_{2,\max}], \text{ if } H_2(z) = 0. \end{cases}$

Along any extremal, if the control $u(\cdot)$ belongs to the interior of the control domain U then the *Legendre-Clebsch* condition

$$\frac{\partial^2 H}{\partial u^2}(z(t), u(t), \eta(t))(v, v) \leqslant 0, \quad \forall v \in \mathbb{R}^2, \quad \forall t \in [0, t_f],$$

must be satisfied, *i.e.* $H_3(z(t)) \leqslant 0$ for all t in $[0, t_f]$.

3.5. Computations of controls, multipliers and junction conditions (one state constraint)

We only analyze cases we encounter in the numerical experiments. Hence, we focus our study on a scalar state constraint c. We call η its associated multiplier.

Definition 2. A *boundary arc* associated to a state constraint c, is an arc $\gamma_c\colon t \mapsto \gamma_c(t)$ defined on an interval $J = [t_1, t_2]$, not reduced to a singleton, such that $c(\gamma_c(t)) = 0$ for all t in J.

Definition 3. We define the order m of the constraint c as the first integer such that a control variable appear after the m-th differentiation of c with respect to time.

3.5.1. General results

Lemma 3.2. *The state constraints c_γ and c_v are of order 1.*

Proof
The derivative of ψ is

$$\dot{\psi} = \frac{\partial \psi}{\partial x_1}\dot{x}_1 + \frac{\partial \psi}{\partial x_3}\dot{x}_3 = \frac{\partial \psi}{\partial x_1}\dot{x}_1 + \frac{\partial \psi}{\partial x_3}\left(-\omega_6\theta_3 - \omega_2\sin(x_5) + u_1\frac{\theta_1}{x_4} - u_2^2\omega_7\theta_3\right) \tag{11}$$

and so $c_v = \psi - \psi_{\max}$ is of order 1. Since $\dot{c}_\gamma = \dot{x}_5 = -\frac{\omega_2}{x_3}\cos(x_5) + u_2\frac{\theta_3(x,\omega)}{x_3}$, c_γ is of order 1. □

Lemma 3.3. *The partial derivatives of ψ are equal to:*

$$\frac{\partial \psi}{\partial x_1}(x) = \frac{x_3\omega_{12}}{\theta_4\sqrt{\omega_{10}\omega_{12}\theta_4}} = \frac{\omega_{12}}{2\theta_4}\psi(x) \quad \textit{and} \quad \frac{\partial \psi}{\partial x_3}(x) = \frac{1}{\sqrt{\omega_{10}\omega_{12}\theta_4}} = \frac{\psi(x)}{x_3}.$$

We present now the general framework used to parameterize extremals with state constraints c of order 1. Since c is of order 1, we could write in a generic way, $\dot{c} = a_0 + u_1 a_1 + u_2 a_2 + u_2^2 a_3$ with $(a_1, a_2, a_3) \neq (0, 0, 0)$ and with a_0, a_1, a_2 and a_3 depending on x.

Lemma 3.4. *Along the boundary, $\{H, H_i\} = H_{0i} + u_1 H_{1i} + u_2 H_{2i} + u_2^2 H_{3i} - \eta c' f_i$, $i = 0, \ldots, 3$.*

Proof
Computing, $\{H, H_i\} = H_{0i} + u_1 H_{1i} + u_2 H_{2i} + u_2^2 H_{3i} + \{\eta c, H_i\}$, with $\{\eta c, H_i\} = c\{\eta, H_i\} - \eta c' f_i = -\eta c' f_i$ as $c = 0$ and $\frac{\partial c}{\partial p} = 0$. □

Lemma 3.5. *Let consider f_ν a smooth vector field, $H_\nu = \langle p, f_\nu\rangle$ its Hamiltonian lift and τ a junction time. Then we have $\nu_\tau c'(x(\tau))f_\nu(x(\tau)) = H_\nu(z(\tau^-)) - H_\nu(z(\tau^+))$ at the junction point.*

Proof
From eq. (9), we have $p(\tau^+) = p(\tau^-) - \nu_\tau c'(x(\tau))$ at the junction time τ. Multiplying by f_ν leads to $H_\nu(z(\tau^+)) = H_\nu(z(\tau^-)) - \nu_\tau c'(x(\tau))f_\nu(x(\tau))$. □

Lemma 3.6. *Let assume that $\varphi_1 > 0$ and $\varphi_2 = 0$ holds along the boundary arc. Then we have:*

1. *if $(a_2, a_3) = (a_2, 0)$ with $a_2 \neq 0$ then the control $u(x)$ is given by*

$$u(x) = \left(u_{1,\max}, -\frac{a_0 + u_{1,\max}\, a_1}{a_2}\right).$$

2. *if $(a_2, a_3) = (0, a_3)$ with $a_3 \neq 0$ and $a_3(a_0 + u_{1,\max}\, a_1) < 0$ then the control $u(x)$ is given by*

$$u(x) = \left(u_{1,\max}, \sqrt{-\frac{a_0 + u_{1,\max} a_1}{a_3}}\right).$$

And in both cases, the multiplier η associated to the constraint c is defined by

$$\eta = \frac{1}{c'(f_2 + 2u_2 f_3)}\Big(H_{02} + u_{1,\max}(H_{12} + 2u_2 H_{13}) + 2u_2 H_{03} + u_2^2 H_{23} + 2H_3 u_2' f\Big).$$

Remark 3. If $\varphi_1 < 0$, then replace $u_{1,\max}$ by $u_{1,\min}$ in lemma 3.6.

Proof
Since $\varphi_1 > 0,\ u_1 = u_{1,\max}$. Along the boundary $\dot{c} = a_0 + u_{1,\max}a_1 + u_2 a_2 + u_2^2 a_3 = 0,\ u_2 \geqslant 0$, and we determine u_2 in feedback form by solving this equation. Differentiating φ_2 with respect to time and with lemma 3.4, we have along the boundary arc

$$\dot{\varphi}_2 = H_{02} + u_{1,\max}(H_{12} + 2u_2 H_{13}) + 2u_2 H_{03} + u_2^2 H_{23} + 2H_3 u_2' f - \eta c'(f_2 + 2u_2 f_3) = 0.$$

Since c is of order 1, $c'(f_2 + 2u_2 f_3)$ never vanishes along the boundary arc, whence the result. □

Let define now the Hamiltonian $\bar{H}$ depending only on the scalar control u_2 (u_1 is fixed):

$$\bar{H}(x, p, u_2, \eta) \coloneqq H(x, p, (u_{1,\max}, u_2), \eta) = \bar{H}_0 + u_2 H_2 + u_2^2 H_3 + \eta c,$$

where $\bar{H}_0 = H_0 + u_{1,\max}H_1$. The following lemma is due to [4, proposition 2.5].

Lemma 3.7. *Let $(x(\cdot), p(\cdot), u_2(\cdot), \eta(\cdot))$ denote an extremal associated to $\bar{H}$ defined on $[0, t_f]$, satisfying $\frac{\partial \bar{H}}{\partial u_2}(x(t), p(t), u_2(t), \eta(t)) = 0$, $t \in [0, t_f]$, and assume that:*

- $\exists \alpha > 0,\ \dfrac{\partial^2 \bar{H}}{\partial^2 u_2}(x(t), p(t), u_2(t), \eta(t)) < \alpha$ *a.e. on* $[0, t_f]$ *(strict Legendre-Clebsch condition).*
- *the constraint c is of order* 1 *and* $\exists \beta > 0,\ |\dfrac{\partial \dot{c}}{\partial u_2}(x(t), u_2(t))| \geqslant \beta,\ \forall t \in [0, t_f]$.
- *the trajectory has a finite set of junction times.*

Then u_2 is continuous over $[0, t_f]$ and $\nu_\tau = 0$.

3.5.2. Application to problem ($\mathcal{P}_\alpha$)

Extremals in $\mathcal{C}_\gamma = \{x \in M,\ c_\gamma(x) = 0,\ c_v(x) \neq 0\}$. Under assumptions from lemma 3.6, since $\dot{c}_\gamma = \frac{\omega_2}{x_3}\cos(x_5) - u_2\frac{\theta_3}{x_3}$ with $\frac{\theta_3}{x_3} \neq 0$, we have

$$u_1 = \begin{cases} u_{1,\max}, \text{ if } \varphi_1 > 0, \\ u_{1,\min}, \text{ if } \varphi_1 < 0, \end{cases}$$

$$u_{2,\gamma} \coloneqq \frac{\omega_2}{\theta_3}\cos(x_{5,\min}),$$

$$\eta_\gamma \coloneqq -\frac{x_3}{\theta_3}\Big(H_{02} + u_1(H_{12} + 2u_2 H_{13}) + 2u_2 H_{03} + u_2^2 H_{23} + 2H_3 u_2' f\Big),$$

$$\nu_\tau = -\frac{\varphi_2(\tau^-)x_3}{\theta_3} \text{ at the entry point, } \nu_\tau = \frac{\varphi_2(\tau^+)x_3}{\theta_3} \text{ at the exit point.}$$

Extremals in $\mathcal{C}_v = \{x \in M,\ c_\gamma(x) \neq 0,\ c_v(x) = 0\}$. Under assumptions from lemma 3.6, since $\dot{c}_v = \dot{\psi}$ with $\frac{\omega_7\theta_3}{x_3}\psi(x) \neq 0$, we have

$$u_1 = \begin{cases} u_{1,\max}, \text{ if } \varphi_1 > 0, \\ u_{1,\min}, \text{ if } \varphi_1 < 0, \end{cases}$$

$$u_{2,v} \coloneqq \sqrt{\frac{1}{\omega_7\theta_3}\left(\left(\frac{x_3^2\omega_{12}}{2\theta_4} - \omega_2\right)\sin(x_5) - \omega_6\theta_3 + u_1\frac{\theta_1}{x_4}\right)},$$

$$\eta_v \coloneqq -\frac{1}{2u_2\omega_7\theta_3\frac{\partial\psi}{\partial x_3}}\left(H_{02} + u_1\left(H_{12} + 2u_2 H_{13}\right) + 2u_2 H_{03} + u_2^2 H_{23} + 2u_2' f H_3\right),$$

$$\nu_\tau = -\frac{\varphi_2(\tau^-)}{2u_2\omega_7\theta_3\frac{\partial\psi}{\partial x_3}} \text{ at the entry point, } \nu_\tau = \frac{\varphi_2(\tau^+)}{2u_2\omega_7\theta_3\frac{\partial\psi}{\partial x_3}} \text{ at the exit point.}$$

4. NUMERICAL METHODS AND RESULTS

In this section, we present numerical methods used to solve problem $(\mathcal{P}_\alpha)$. Two different types of methods are used in this study, direct and indirect methods (shooting techniques). The indirect methods are implemented within the *HamPath* package [6]. Since in the constraint case the control is piecewise smooth, multiple shooting is necessary to concatenate different smooth arcs and moreover on each smooth arc to deal with numerical instability [19]. Direct methods, within the *Bocop* software [3], are used first to determine the structure of the BC-extremal (see definition 1) and to initialize the multiple shooting method.

The *Bocop* software tranforms an infinite dimensional optimal control problem (OCP) into a finite dimensional optimization problem called Non Linear Problem (NLP). Full time discretization is applied to state and control variables. These techniques are generally less precise than indirect methods, but there are more robust with respect to initialization. The discretized problem from *Bocop* is solved using the interior point solver *Ipopt* [20] with *MUMPS* [1] and all the derivatives are computed using automatic differentiation with *ADOL-C* software [21].

For the multiple shooting problem solved by *HamPath*, the Fortran hybrid Newton method *hybrj* [15] is used to solve the non linear system and all the derivatives are computed using automatic differentiation with *tapenade* software [11].

4.1. Numerical methods

First of all, the following technical result justify the use of direct method to initialize the shooting technique.

4.1.1. A link between KKT conditions and the maximum principle with state constraints

The optimal control problem is transformed into a fixed final time one ($t = s\,t_f$, $s \in [0,1]$):

$$(\mathcal{P}_\alpha)\begin{cases} \min g(t_f(1), x(1)) \\ \dot{x}(s) = t_f(s)\, f(x(s), u(s)) \\ \dot{t}_f(s) = 0 \\ x(0) = x_0 \ \text{ fixed} \\ c(x(s)) \leqslant 0 \\ c_u(u(s)) = (u_1(s) - u_{1,\max},\ -u_1(s) + u_{1,\min},\ u_2(s) - u_{2,\max},\ -u_2(s) + u_{2,\max}) \leqslant 0. \\ b(x(1)) = 0 \end{cases}$$

The Hamiltonian associated to this optimal control problem is then

$$H(x, t_f, u, p, p_{t_f}, \eta) = \langle t_f\, f(x,u), p\rangle + \langle \eta, c(x)\rangle,$$

and the lagrangian associated to the Non Linear Problem (NLP) obtained by the discretization of the state equation by implicit Euler scheme is using the notation here $x = (x_1, \ldots, x_N)$, $u = (u_1, \ldots, u_N)$, $p = (p_0, \ldots, p_{N-1})$, $\mu = (\mu_1, \ldots, \mu_N)$ and $\tilde{\eta} = (\tilde{\eta}_1, \ldots, \tilde{\eta}_N)$

$$\begin{aligned} L(x, t_f, u, p, \mu, \tilde{\eta}, \lambda) = \ & g(t_f, x_N) + \sum_{i=0}^{N-1} \langle p_i, x_{i+1} - x_i - h t_f f(x_{i+1}, u_{i+1})\rangle \\ & + \sum_{i=1}^{N} \langle \mu_i, c_u(u_i)\rangle + \sum_{i=1}^{N} \langle \tilde{\eta}_i, c(x_i)\rangle + \langle \lambda, b(x_N)\rangle. \end{aligned}$$

We have then the following proposition.

Proposition 4.1. *If the maximization of the Hamiltonian is equivalent to its Karush-Kuhn-Tucker conditions and furnishes us the optimal control as a function of the state and adjoint state $u(x, t_f, p)$, then the (KKT) necessary conditions of the (NLP) problem are equivalent to*

1. *The discretization of the adjoint state equation by explicit Euler scheme*

$$\begin{aligned} p_i &= p_{i-1} - h\frac{\partial H}{\partial x}(x_i, t_{f,i}, u_i, p_{i-1}, p_{t_f,i-1}, \eta_i) + \eta_i c_x'(x_i),\ (\eta_i \coloneqq \tilde{\eta}_i h) \\ p_{t_f,i} &= p_{t_f,i-1} - h\langle f(x_i, u_i), p_{i-1}\rangle. \end{aligned}$$

2. *The maximization of the Hamiltonian*

$$\begin{cases} \max H(x_i, t_f, u_i, p_{i-1}, p_{t_f,i-1}, \eta_i) \\ c_u(u_i) \leqslant 0. \end{cases}$$

3. *The transversality conditions*

$$\begin{aligned} p_N &= -\frac{\partial g}{\partial x}(t_f, x_N) - \lambda b'(x_N) \\ p_{t_f,N} &= -\frac{\partial g}{\partial t_f}(t_f, x_N). \end{aligned}$$

4. $c(x_i) \leqslant 0$, $\eta_i \leqslant 0$, $\langle \eta_i, c(x_i)\rangle = 0 \ \ for \ \ i = 1, \ldots, N$
5. $b(x_N) = 0$.

Proof
For the adjoint equation and the transversality conditions the result immediately follows from

$$\frac{\partial L}{\partial x_i}(x, t_f, u, p, \mu, \tilde{\eta}, \lambda) = 0 \ \text{ and } \ \frac{\partial L}{\partial t_f}(x, t_f, u, p, \mu, \tilde{\eta}, \lambda) = 0.$$

For the maximization of the Hamiltonian we compute

$$\frac{\partial L}{\partial u_i}(x, t_f, u, p, \mu, \tilde{\eta}, \lambda) = -h\, t_f \frac{\partial f}{\partial u}(x_i, u_i) p_{i-1} + c_u'(u_i)\mu_i = 0 \ \text{ for } \ i = 1, \ldots, N.$$

Then, if we add the conditions $c_u(u_i) \leqslant 0$, $\mu_i \leqslant 0$ and $\langle \mu_i,\, c_u(u_i)\rangle = 0$, we recognize the (KKT) conditions of the maximization of the Hamiltonian. □

Remark 4. In the unconstrained case and if we don't have constraints on the control, this result is well known [5, 7, 8, 9, 14] and the scheme Figure 5 commutes.

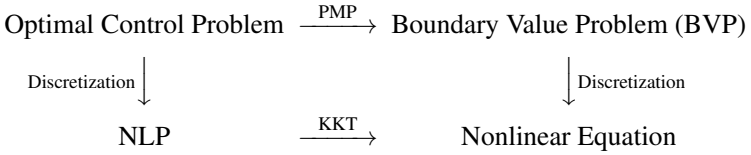

Figure 5. *This scheme commutes if the discretization of the state-adjoint state equation is a partitioned Runge-Kutta and symplectic scheme [10].*

Remark 5. An important point is here that if we want to compute the optimal control from the state and adjoint state variables, we have to compute $u(x_i, p_{i-1})$ and not $u(x_i, p_i)$. See also Figure 6 to observe the difference between the Lagrange multipliers associated to the state constraint in the two cases: KKT on the NLP problem and discretization of the BVP problem.

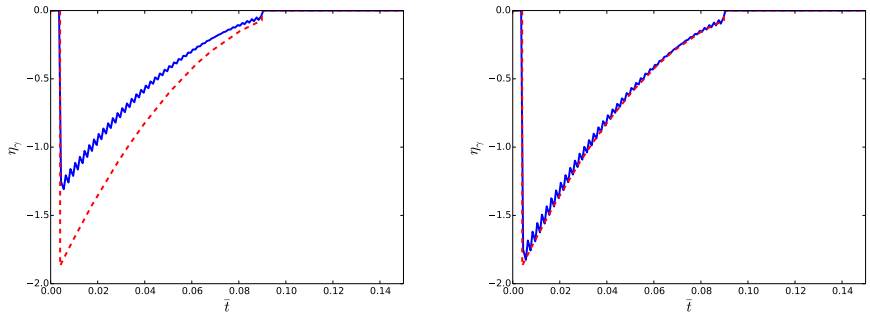

Figure 6. Evolution of the multiplier η_γ associated to the constraint c_γ. The solid blue lines represent the data extracted from direct method. Data in the rough ($\tilde{\eta}_i$) are presented on the left figure whereas processed data ($\eta_i = \tilde{\eta}_i h$, with h the step size) are presented on the right figure. The red dashed lines represent the multiplier from the discretization of the BVP problem (obtained with indirect method).

4.1.2. Hamiltonian associated to the constrained arc

Proposition 4.2. *Let $c(x) \leqslant 0$ be a scalar constraint of order 1. We define for $z \coloneqq (x,p) \in T^*M$ the Hamiltonian*

$$\bar{H}_\mathcal{C}(z) \coloneqq \bar{H}(z, u_2(x), \eta(z)) = H_0(z) + u_{1,\max} H_1(z) + u_2(x) H_2(z) + u_2(x)^2 H_3(z) + \eta(z)\, c(x)$$

with u_2 and η given in section 3.5.2. Let $\tilde{z} \coloneqq (\tilde{x}, \tilde{p})$ such that $\varphi_2(\tilde{z}) = 0$ and $c(\tilde{x}) = 0$. Assuming $\varphi_1 > 0$, then there is exactly one extremal passing through $\tilde{z}$, such that $c = 0$ and $\varphi_2 = 0$ along the extremal, and it is defined by the flow of $\bar{H}_\mathcal{C}$.

Proof
First we show that the space $\Sigma \coloneqq \{(x,p) \in T^*M, c(x) = 0, \varphi_2(x,p) = 0\}$ is invariant with respect to the flow of $\bar{H}_c$. Let $z(\cdot) \coloneqq (x(\cdot), p(\cdot))$ be the integral curve of $\bar{H}_c$ passing through $\tilde{z} \coloneqq (\tilde{x}, \tilde{p}) \in \Sigma$ at time $t = 0$. Let define $\Gamma \coloneqq (\Gamma_1, \Gamma_2) \circ z(\cdot)$ with $\Gamma_1 \coloneqq c \circ \pi_x$ and $\Gamma_2 \coloneqq H_2 + 2(u_2 \circ \pi_x) H_3$, with $\pi_x(x,p) = x$. For readibility, we note c (resp. u_2) instead of $c \circ \pi_x$ (resp. $u_2 \circ \pi_x$) in the following calculus. Since Γ is differentiable, we have

$$\begin{aligned}
\frac{\mathrm{d}\Gamma_1 \circ z}{\mathrm{d}t}(t) =& \{\bar{H}_\mathcal{C}, \Gamma_1\}(z(t)) \\
=& \Big(\underbrace{c'\, f}_{=0, \text{ definition of } u_2} + (H_2 + 2u_2 H_3) \underbrace{\{u_2, \Gamma_1\}}_{=0} + \Gamma_1 \{\eta, \Gamma_1\} \Big)(z(t)) \\
\frac{\mathrm{d}\Gamma_2 \circ z}{\mathrm{d}t}(t) =& \{\bar{H}_\mathcal{C}, \Gamma_2\}(z(t)) \\
=& \Big(\underbrace{H_{02} + u_{1,max}(H_{12} + 2u_2 H_{13}) + 2u_2 H_{03} + u_2^2 H_{23} + 2H_3 u_2' f}_{= \eta c'(f_2 + 2u_2 f_3), \text{ by definition of } \eta} \\
& - \eta c'(f_2 + 2u_2 f_3) + \Gamma_2(\{u_2, H_2\} + 2u_2\{u_2, H_3\}) + \Gamma_1\{\eta, \Gamma_2\} \Big)(z(t))
\end{aligned}$$

Then $\dot{\Gamma}(t) = A(t)\Gamma(t)$, with $A(t) = \begin{pmatrix} \{\eta, \Gamma_1\} & 0 \\ \{\eta, \Gamma_2\} & \{u_2, H_2\} + 2u_2\{u_2, H_3\} \end{pmatrix}(z(t))$. Since $\Gamma(0) = 0$, $\Gamma \equiv 0$ and then $z(\cdot)$ remains in Σ. Besides,

$$\bar{H}'_\mathcal{C}(z) = \frac{\partial \bar{H}}{\partial z}(z, u_2(x), \eta(z)) + \frac{\partial \bar{H}}{\partial u_2}(z, u_2(x), \eta(z))\, u_2'(x) + \frac{\partial \bar{H}}{\partial \eta}(z, u_2(x), \eta(z))\, \eta'(z)$$

with

$$\frac{\partial \bar{H}}{\partial u_2}(z, u_2(x), \eta(z)) = \Gamma_2(z), \quad \frac{\partial \bar{H}}{\partial \eta}(z, u_2(x), \eta(z)) = \Gamma_1(z).$$

So $\vec{\bar{H}}_\mathcal{C}(z(t)) = \vec{\bar{H}}(z(t))$ as Γ_1 and Γ_2 vanish along $z(\cdot)$ and $(z(\cdot), (u_{1,max}, u_2 \circ x(\cdot)), \eta \circ z(\cdot))$ is extremal. □

4.1.3. Multiple shooting method

We define

$$\begin{aligned}
H_+(z) &\coloneqq H(z,(u_{1,\max},\bar{u}_2(z)),0),\\
H_-(z) &\coloneqq H(z,(u_{1,\min},\bar{u}_2(z)),0),\\
H_\gamma(z) &\coloneqq H(z,(u_{1,\max},u_{2,\gamma}(z)),\eta_\gamma(z)),\\
H_v(z) &\coloneqq H(z,(u_{1,\max},u_{2,v}(z)),\eta_v(z)).
\end{aligned}$$

the different true Hamiltonians related to the unconstrained cases (H_+, H_-), see section 3.4, and to the constrained cases (H_γ, H_v), see section 3.5.2. We define also the mapping $\exp\colon (t,z_0)\mapsto \exp(t\vec{H})(z_0)$ which gives the solution at the time t of the Cauchy problem $\dot{z}(s)=\vec{H}(z(s))$, $z(0)=z_0$. We note $\sigma_1\sigma_2$ an arc σ_1 followed by an arc σ_2, σ_i denoting the projection $\pi_x(\exp(t\vec{H}_i)(z_0))$ with $H_i\in\{H_+,\,H_-,\,H_\gamma,\,H_v\}$.

The unconstrained case. We consider that we have only one unconstrained arc of the form σ_+. On this single arc, we need multilple shooting technique to deal with numerical instability. We note (z_i,t_i) the discretized points and times for multiple shooting. The times t_i are fixed and defined by $t_{i+1}=t_i+\Delta t$, $i=0,\dots,N-1$ with $\Delta t=t_f/(N+1)$. Then the multiple shooting function

$$S_1(p_0,t_f,z_1,\cdots,z_N)$$

is given by the following equations.

$$\begin{aligned}
x_{1,f}&=\pi_{x_1}(z(t_f,t_N,z_N)),\quad x_{2,f}=\pi_{x_2}(z(t_f,t_N,z_N)),\\
x_{3,f}&=\pi_{x_3}(z(t_f,t_N,z_N)),\quad x_{5,f}=\pi_{x_5}(z(t_f,t_N,z_N)),\\
(\alpha-1)p^0&=\pi_{p_4}(z(t_f,t_N,z_N)),\quad -\alpha p^0=H_+(z(t_f,t_N,z_N)),\\
0&=z(t_1,t_0,z_0)-z_1,\quad 0=z(t_2,t_1,z_1)-z_2,\quad \dots,\quad 0=z(t_N,t_{N-1},z_{N-1})-z_N,
\end{aligned}$$

where $z_0\coloneqq(x_0,p_0)$, $z\colon (t_1,t_0,z_0)\mapsto\exp((t_1-t_0)\vec{H}_+)(z_0)$. A zero of S_1 gives a BC-extremal which satisfies the necessary conditions of the maximum principle defined in section 3.

The constrained case. We consider an extremal of the form $\sigma_+\sigma_\gamma\sigma_+$ and we note $t_1<t_2$ the switching times. From proposition 4.2 we only need to check $c_\gamma=0$ and $\varphi_2=0$ at the entry-time of the boundary arc, *i.e* $c_\gamma(x(t_1))=0$ and $H_2(z(t_1))+2u_{2,\gamma}(x(t_1))H_3(z(t_1))=0$. From lemma 3.7, the jumps at times t_1 and t_2 are zero, *i.e.* $\nu_{t_1}=\nu_{t_2}=0$. Due to numerical instability, mutliple shooting is also used on $[t_2,t_f]$ with $(t_{s,i},z_{s,i})$ the discretized points and times (with $t_{s,0}=t_2$) such that $t_{s,i+1}=t_{s,i}+\Delta t$ for $i=0,\dots,N-1$ with $\Delta t=(t_f-t_2)/(N+1)$. In this case, the multiple shooting function

$$S_2\coloneqq(p_0,t_1,t_2,t_f,z_1,z_2,z_{s,1},\dots,z_{s,N})$$

is given by the following equations.

$$\begin{aligned}
0&=c_\gamma(\pi_x(z_1)),\quad 0=H_2(z_1)+2u_{2,\gamma}(\pi_x(z_1))H_3(z_1),\\
x_{1,f}&=\pi_{x_1}(z(t_f,t_{s,N},z_{s,N})),\quad x_{2,f}=\pi_{x_2}(z(t_f,t_{s,N},z_{s,N})),\\
x_{3,f}&=\pi_{x_3}(z(t_f,t_{s,N},z_{s,N})),\quad x_{5,f}=\pi_{x_5}(z(t_f,t_{s,N},z_{s,N})),\\
(\alpha-1)p^0&=\pi_{p_4}(z(t_f,t_{s,N},z_{s,N})),\quad -\alpha p^0=H_+(z(t_f,t_N,z_{s,N})),\\
0&=z(t_1,t_0,z_0)-z_1,\quad 0=\exp((t_2-t_1)\vec{H}_\gamma)(z_1)-z_2,\quad 0=z(t_{s,1},t_2,z_2)-z_{s,1},\\
0&=z(t_{s,2},t_{s,1},z_{s,1})-z_{s,2},\ \dots,\quad 0=z(t_{s,N},t_{s,N-1},z_{s,N-1})-z_{s,N},
\end{aligned}$$

where $z_0\coloneqq(x_0,p_0)$, $z\colon (t_1,t_0,z_0)\mapsto\exp((t_1-t_0)\vec{H}_+)(z_0)$. A zero of S_2 gives a BC-extremal satisfying the necessary conditions from section 3 and of the form $\sigma_+\sigma_\gamma\sigma_+$.

4.2. Numerical results

4.2.1. The problem ($\mathcal{P}_1$)

The unconstrained case. The shooting function S_1 defined in section 4.1.3 is implemented with data from Table III, $N = 16$ arcs and an initial mass of $x_{0,4} = 72\ 000$ kg. The Newton method algorithm used to find a zero of S_1 is initialized by data coming from direct methods (*Bocop*) and presented in section 2.3. The resulting unconstrained trajectory reaches the final manifold in $t_f = 696$ s and the aircraft consumed 964 kg of fuel. The corresponding states, adjoints, controls and constraints are displayed with solid lines on Figures 7 and 8. Let focus on Figure 7, the behavior of the altitude h and of the speed v are opposed at the beginning and at the end of the trajectory. At the beginning, the aicraft trades potential energy for kinetic energy in order to reach a sufficient climbing speed and at the end of the trajectory, the opposite exchange is realized in order to reach the targeted altitude. We can summarize this behaviour as an energy sharing strategy and even though this strategy fulfills the constraint c_v, it violates the constraint c_γ.

The constrained case. The result from direct method with the constraint on γ is given in the preliminary section 2.3, in Figure 3. From this figure, we deduce that the trajectory σ^* is composed by a concatenation of constrained and unconstrained arc such that $\sigma^* \coloneqq \sigma_+\sigma_\gamma\sigma_+$. The shooting function S_2 defined in section 4.1.3 is then implemented with data from Table III, $N = 17$ arcs and an initial mass of $x_{0,4} = 72\ 000$ kg. As for the unconstrained case, the Newton method used to find a zero of S_2 is initialized by data from *Bocop*. The resulting trajectory reaches the targeted manifold in $t_f = 698$ s which is slighty superior than the unconstrained case but the aircraft still consumes around 964 kg of fuel. The red dashed lines on Figures 7 and 8 represent the constrained trajectory. The energy sharing strategy is used here at the end of the trajectory to gain potential energy and reach the targeted manifold.

4.2.2. The problem ($\mathcal{P}_{0.6}$)

The unconstrained case. The result from direct method for the problem $(\mathcal{P}_\alpha)$ with $\alpha = 0.6$ in the unconstrained case is given in Figure 4 (solid lines). From this figure, the trajectory is of the form $\sigma^* \coloneqq \sigma_+\sigma_-$. In this case, the shooting function is clear. The difference from S_1 comes from the switching between σ_+ and σ_-. An additional condition is given by $H_1 = 0$ at the switching time t_1 which is an unknown of the shooting function in this case. This new function is then implemented using data from Table III, $N = 15$[¶] and with an initial mass of $x_{4,0} = 59\ 000$ kg. The data from *Bocop* are still used as an initial guess for the shooting method. The trajectory represented on Figures 9 and 10 by the blue solid lines is quite similar to the unconstrained case of the problem $(\mathcal{P}_1)$. It reaches the targeted manifold in $t_f = 650$ s with a fuel consumption of 873 kg. The observation of the Figure 10 shows that both constraints c_γ and c_v are violated by this trajectory but never simultaneously.

The constrained case. We deduce from the figure 4 and the unconstrained case that the trajectory is a concatenation of constrained and unconstrained arc such that $\sigma^* \coloneqq \sigma_+\sigma_\gamma\sigma_+\sigma_v\sigma_-$. The corresponding shooting function is then adapted from the shooting function S_2 and is implemented using data from Table III and an initial mass of $x_{4,0} = 59\ 000$ kg. We split the second arc σ_+ and the arc σ_v in $N_+ = 12$ and $N_v = 10$ subarcs in order to deal with numerical instabilities. Like the other cases, data from *Bocop* are used as an initial guess to find a zero of the shooting function. The red dashed lines of Figures 9 and 10 depict the resulting trajectory. The final time $t_f = 654$ s is slightly superior than the final time in the unconstrained case, whereas the fuel consumption of 869 kg is slighty inferior. As for the problem $(\mathcal{P}_1)$, the constrained trajectory from $(\mathcal{P}_{0.6})$ follows the unconstrained one and the boundaries arcs do not modify the global behavior of the trajectory.

[¶]The multiple shooting technique is only used along σ_+ since the arc σ_- is short.

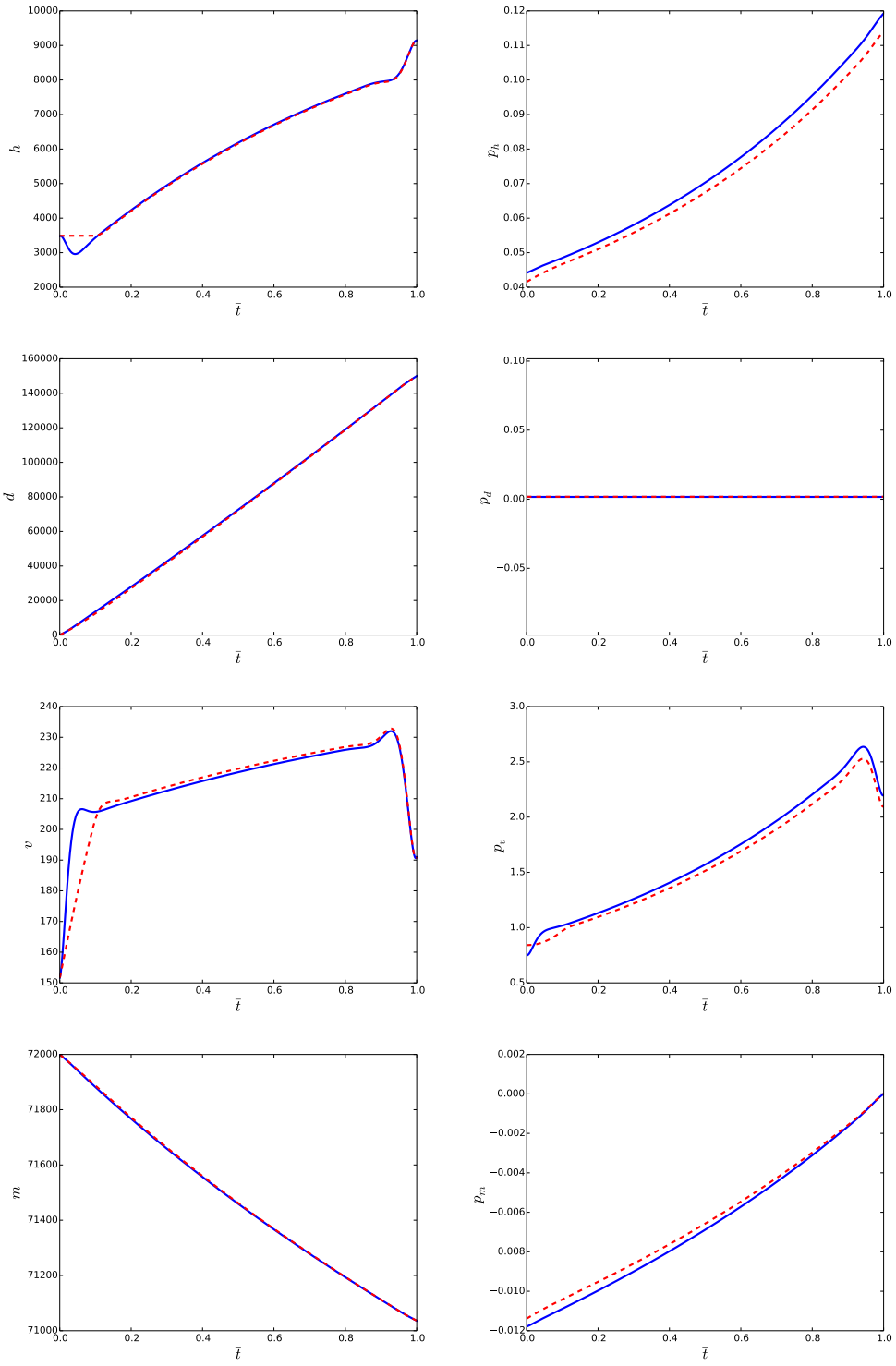

Figure 7. **Problem** ($\mathcal{P}_1$)**.** Evolution of the state (left) and adjoint (right) variables along the state unconstrained (blue plain lines) and the state constrained (red dashed lines) trajectories in the time minimal case with respect to the normalized time $\bar{t}$. From top to the bottom, we display the altitude h, the longitudinal distance d, the speed v and the mass m.

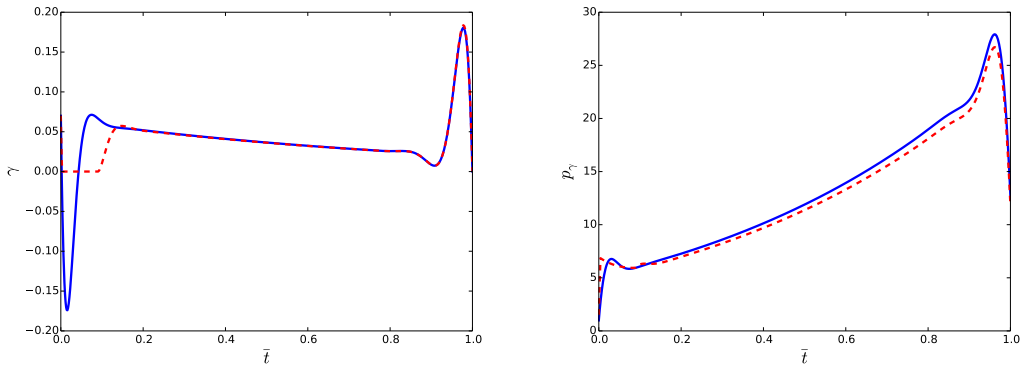

Figure 7. **Problem ($\mathcal{P}_1$).** Evolution of the air slope γ (left) and its associated adjoint p_γ (right) along the state unconstrained (blue solid lines) and the state constrained (red dashed line) trajectories with respect to the normalized time $\bar{t}$.

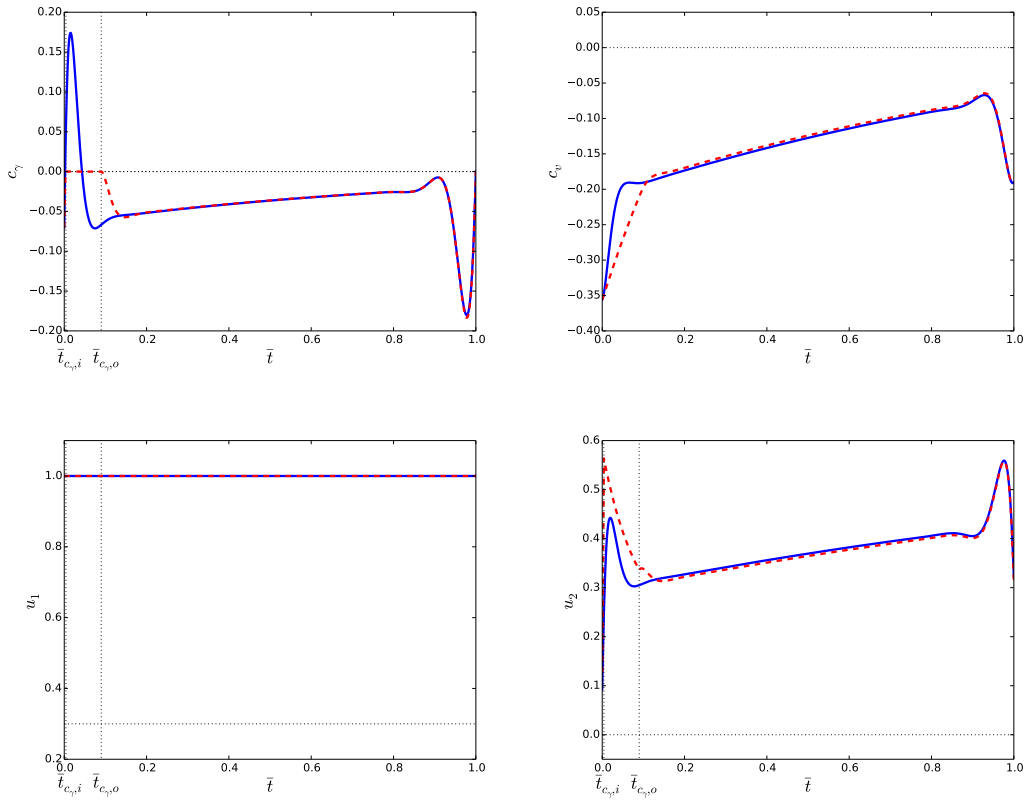

Figure 8. **Problem ($\mathcal{P}_1$).** Evolution of the constraints and the controls along the state unconstrained (blue solid lines) and state constrained (red dashed lined) trajectories with respect to the normalized time $\bar{t}$, in the time minimal case. From top left to bottom right, the constraint on the air slope (c_γ), the constraint on MACH speed (c_v), the thrust ratio (u_1) and the lift coefficient (u_2) are displayed. The time $\bar{t}_{c_\gamma,i}$ (resp. $\bar{t}_{c_\gamma,o}$) represents the entry (resp. the exit) time on the constraint c_γ. The horizontal black dotted lines represents the bounds of the constraints on the state and the control.

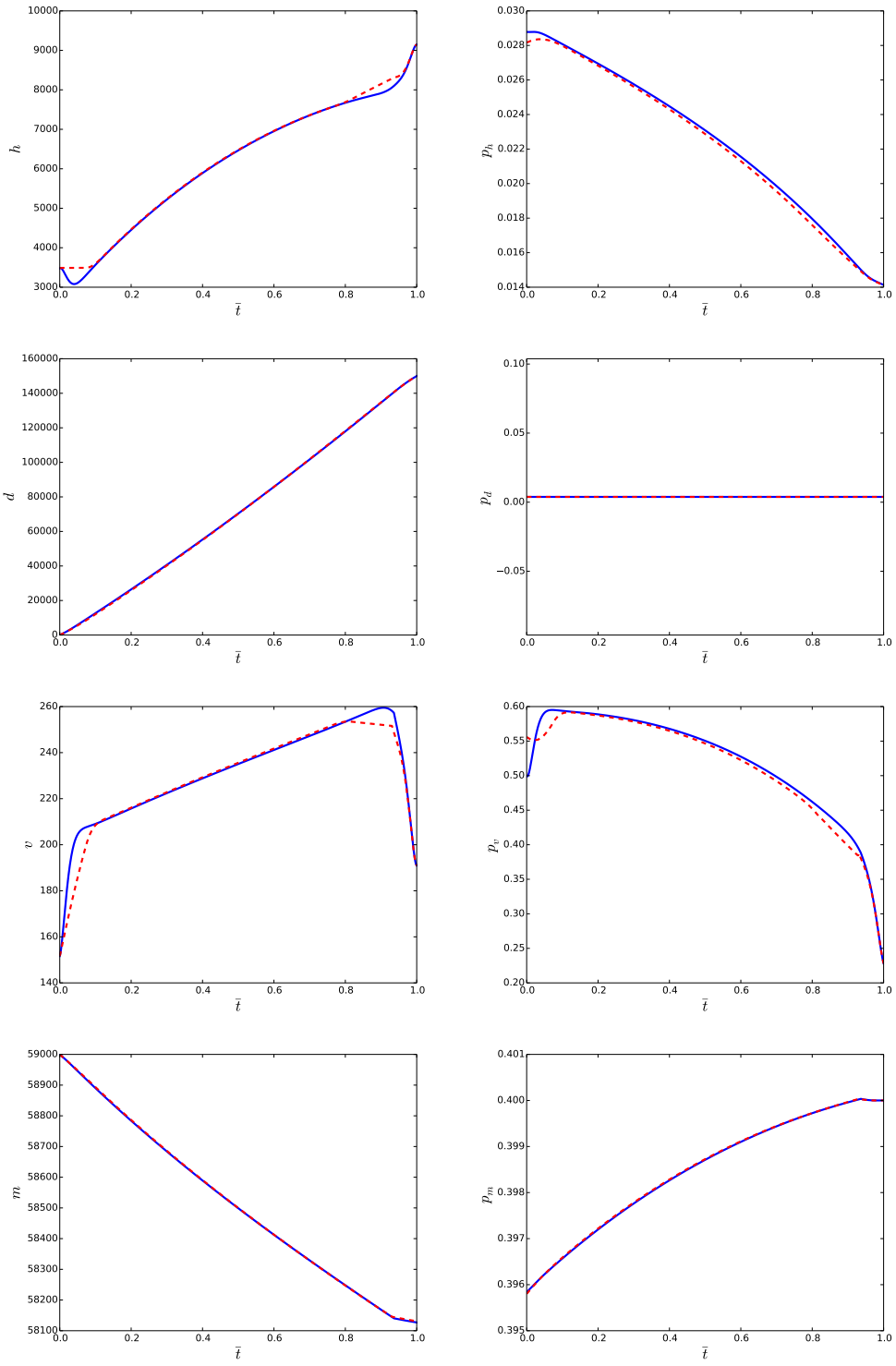

Figure 9. **Problem ($\mathcal{P}_{0.6}$).** Evolution of the state (left) and adjoint (right) variables along the state unconstrained (blue plain lines) and the state constrained (red dashed lines) trajectories in the mixed criterion problem ($\alpha = 0.6$) with respect to the normalized time $\bar{t}$. From top to the bottom, we display the altitude h, the longitudianl distance d, the speed v and the mass m.

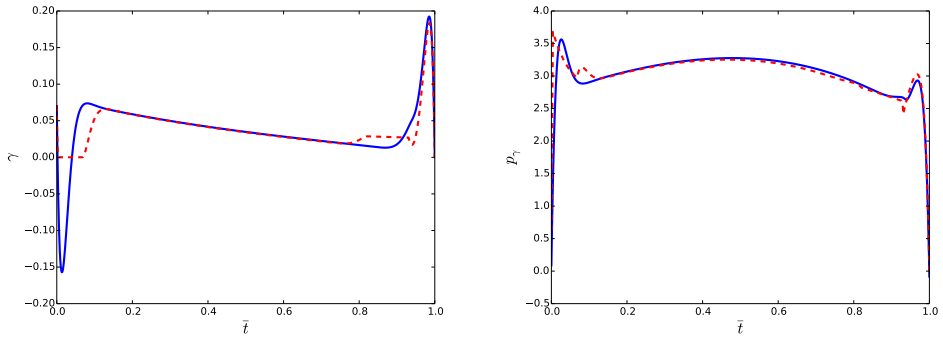

Figure 9. **Problem** ($\mathcal{P}_{0.6}$)**.** Evolution of the air slope γ (left) and its associated adjoint p_γ (right) along the state unconstrained (blue solid lines) and the state constrained (red dashed line) trajectories with respect to the normalized time $\bar{t}$.

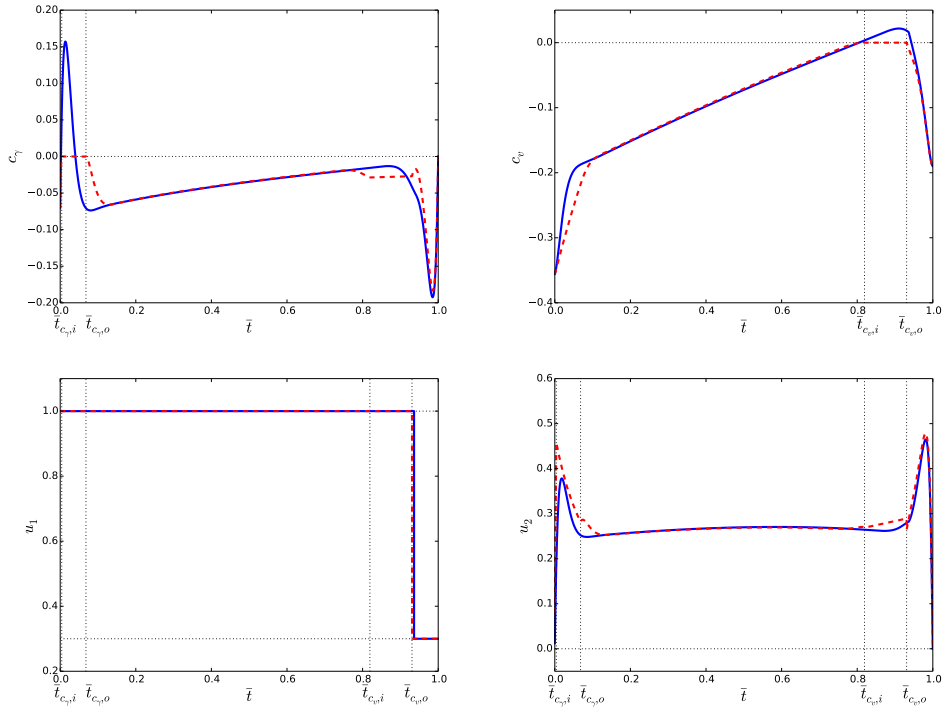

Figure 10. **Problem** ($\mathcal{P}_{0.6}$)**.** Evolution of the constraints and the controls along the state unconstrained (blue solid lines) and state constrained (red dashed lined) trajectories with respect to the normalized time $\bar{t}$ in the mixed criterion problem ($\alpha = 0.6$). From top left to bottom right, the constraint on the air slope (c_γ), the constraint on MACH speed (c_v), the thrust ratio (u_1) and the lift coefficient (u_2) are displayed. The time $\bar{t}_{c_{x,i}}$ (resp. $\bar{t}_{c_{x,o}}$), $x \in \{\gamma, v\}$, represents the entry (resp. the exit) time on the constraint c_x. The horizontal black dotted lines represents the bounds of the constraints on the state and the control.

5. CONCLUSION

In this paper, the control problem of an aircraft in a climbing phase was modeled as a Mayer optimal control problem with two state constraints of order 1 and with affine and quadratic dependance with respect to the control.

We have presented an approach which combines geometric analysis and numerical methods to compute candidates as minimizers which are selected among a set of extremals, solutions of

a Hamiltonian system given by the maximum principle (section 3). The optimal trajectory is a concatenation of boundary and interior arcs. In section 3.5, we compute for each type of arcs we encounter in the numerical experiments, the control law, the multiplier associated to the constraint (scalar of order 1) and the jumps on the adjoint vector at junction times. Then we combined the theoretical results with indirect and direct methods to compute solutions which satisfy necessary conditions of optimality given by the maximum principle. One can find two technical results in section 4.1. First, proposition 4.1 justifies the use of the direct method to initialize the indirect method in the case of state constrained optimal control problems. The second result from proposition 4.2 is a key tool for the definition of the multiple shooting functions which are solved by the indirect method, see section 4.1.3. At the end, we illustrate the approach with two examples: in section 4.2.1, we give a result about the minimum time problem while in section 4.2.2, one can find a more complex trajectory of the form $\sigma_+\sigma_\gamma\sigma_+\sigma_v\sigma_-$ in the case of a mixed criterion between time of flight and fuel consumption.

REFERENCES

1. P. R. Amestoy, I. S. Duff, J. Koster, and J.-Y. L'Excellent. A fully asynchronous multifrontal solver using distributed dynamic scheduling. *SIAM J. Matrix Anal. Appl.*, 23(1):15–41, 2001.
2. M. D. Ardema. Solution of the minimum time-to-climb problem by matched asymptotic expansions. *AIAA Journal*, 14(7):843–850, 1976.
3. F. J. Bonnans, D. Giorgi, V. Grelard, S. Maindrault, and P. Martinon. Bocop - a collection of examples. Technical report, INRIA, july 2014.
4. J. F. Bonnans and A. Hermant. Well-posedness of the shooting algorithm for state constrained optimal control problems with a single constraint and control. *SIAM J. Control Optim.*, 46(4):1398–1430, 2007.
5. J. F. Bonnans and J. Laurent-Varin. Computation of order conditions for symplectic partitioned Runge-Kutta schemes with application to optimal control. Research Report RR-5398, INRIA, 2004.
6. J.-B. Caillau, O. Cots, and J. Gergaud. Differential continuation for regular optimal control problems. *Optim. Methods Softw.*, 27(2):177–196, 2012.
7. A. L. Dontchev, W. Hager, and V. M. Veliov. Second-order Runge-Kutta approximations in constrained optimal control. *SIAM J. Numer. Anal.*, 38(1):202–226, 2000.
8. A. L. Dontchev and W. W. Hager. The Euler approximation in state constrained optimal control. *Math. Comp.*, 70(233):173–203, 2001.
9. W. Hager. Runge-Kutta methods in optimal control and the transformed adjoint system. *Numer. Math.*, 87(2):247–282, 2000.
10. E. Hairer, C. Lubich, and G. Wanner. *Geometric Numerical Integration. Structure–Preserving Algorithms for Ordinary Differential Equations*, volume 31 of *Springer Series in Computational Mathematics*. Springer-Verlag Berlin Heidelberg, second edition, 2006.
11. L. Hascoët and V. Pascual. The Tapenade Automatic Differentiation tool: Principles, Model, and Specification. *ACM Trans. Math. Software*, 39(3), 2013.
12. A. D. Ioffe and V. M. Tikhomirov. *Theory of extremal problems*. Studies in mathematics and its applications. North-Holland Pub. Co. New York, Amsterdam, New York, 1979.
13. D. H. Jacobson, M. M. Lele, and J. L. Speyer. New necessary conditions of optimality for control problems with state-variable inequality constraints. *J. Math. Anal. Appl.*, 35:255–284, 1971.
14. J. Laurent-Varin. *Calcul de trajectoires optimales de lanceurs spatiaux réutilisables par une méthode de point intérieur*. Thèse de doctorat, École Polytechnique, novembre 2005.
15. J. J. Moré, B. S. Garbow, and K. E. Hillstrom. User guide for minpack-1. Technical Report ANL-80-74, Argonne National Library, 1980.
16. N. Nguyen. Singular arc time-optimal climb trajectory of aircraft in a two-dimensional wind field. In *AIAA Guidance, Navigation and Control Conference and Exhibit*, Guidance, Navigation, and Control and Co-located Conferences, august 2006.
17. D. Poles. Base of aircraft data (BADA) aircraft performance modelling report. EEC Technical/Scientific Report 2009-09, Eurocontrol, september 2009.
18. L. Pontriaguine, E. Michtchenko, R. Gamkrelidze, and V. Boltianski. *Théorie mathématique des processus optimaux*. Mir, Moscou, 1974.
19. J. Stoer and R. Bulirsch. *Introduction to Numerical Analysis*, volume 12 of *Texts in Applied Mathematics*. Springer-Verlag New-York, third edition, 2002.
20. A. Wachter and L. T. Biegler. On the implementation of a primal-dual interior point filter line search algorithm for large-scale nonlinear programming. *Math. Program.*, 106(1):25–57, 2006.
21. A. Walther and A. Griewank. Getting started with adol-c. *Combinatorial Scientific Computing, Chapman-Hall CRC Computational Science*, pages 181–202, 2012.